Fusion Engineering and Design 85 (2010) 687–693

Contents lists available at ScienceDirect

Fusion Engineering and Design

journal homepage: www.elsevier.com/locate/fusengdes

Analysis, verification, and benchmarking of the transient thermal hydraulic ITERTHA code for the design of ITER divertor

Salah El-Din El-Morshedy[a,*], Ahmed Hassanein[b]

[a] Atomic Energy Authority, Cairo, Egypt
[b] Purdue University, West Lafayette, IN, USA

ARTICLE INFO

Article history:
Received 2 November 2009
Received in revised form 26 March 2010
Accepted 30 March 2010
Available online 28 April 2010

Keywords:
Thermal hydraulics
Plasma transient events
ITER divertor

ABSTRACT

An analytical study for the International Thermonuclear Experimental Reactor Thermal Hydraulic Analysis code (ITERTHA) is carried out for a copper divertor with a 5 mm tungsten tile. The influence of the incident heat flux, swirl-tape insertion in cooling channels as well as the coolant flow velocity on the divertor thermal response is analyzed and discussed. The ITERTHA code results are verified by the commercial finite element code, COSMOS. The heat transfer coefficients at the nodes located on the cooling channel-wall are determined outside COSMOS code by the same methodology used in ITERTHA. A good agreement is achieved under different incident heat fluxes. The ITERTHA code is also benchmarked against the thermal-hydraulic calculation of the outer divertor of the Fusion Ignition Research Experiment, FIRE for an incident heat flux of 20 MW/m^2 and coolant flow velocity of 10 m/s in a cooling channel of 8 mm diameter with swirl-tape inserts of 2 ratio and 1.5 mm thickness. The results show excellent agreement for both steady and transient states and prove the successful implementation of both the hydraulic and heated diameters of the swirl-tape channels in the used heat transfer correlations.

1. Introduction

The divertor modules in the International Thermonuclear Experimental Reactor (ITER) are used to remove exhaust from the burning plasma and so receive the highest heat loads of the Plasma Facing Components (PFCs). In order to increase the heat removal capability of the divertor, the device may have several individual coolant channels defined as divertor plates that run parallel to each other and are assembled as a unit. The divertor plates usually have protective armour tiles to limit plasma damage to the copper heat sink structure. The divertor plate is subjected to high heat loads on its one side by the plasma. Therefore, Araki et al. [1] performed experiments on heat transfer of smooth and swirl tubes under one-sided heating conditions and proposed a new heat transfer for the subcooled partial nucleate boiling region under one-sided heating condition. Besides, Marshall [2] reports an investigation of the critical heat flux in the subcooled flow boiling regime of water subcooled flow in one-side heated swirl tubes. Their experimental results corresponding to various thermal-hydraulic conditions were reasonably well predicted by a deduced new correlation. On the other hand Boscary et al. [3] analyzed the influence of the finite element peaking factor (FEPF) that converts the heat flux predicted by CHF correlations into a plasma heat flux that can be measured. The analyses illustrated that the FEPF is proportional to the plasma heat flux and thus accurate calculation of the CHF requires the use of the appropriate FEPF for the given water conditions and plasma heat flux.

In the ITER divertor, the selection of the armour material is mainly based on the erosion lifetime assessment and the plasma interaction [4]. Carbon-fiber composites (CFC) material has been selected for the strike point area because it sublimes rather than melting during plasma transient events such as disruption giant edge-localized mode, and vertical displacement events. Tungsten is selected elsewhere due to its low sputtering yield (less plasma impurities) and to limit tritium codeposition effects (safety and operation).

During normal operations, ITER PFCs are expected to absorb an average heat load of 2 MW/m^2 while the divertor plates will be designed to absorb an average heat flux of 5 MW/m^2 [5]. In order to insure reactor reliability, the reactor cooling system needs to be designed to withstand the most probable and highest heat loads from the plasma, with a substantial margin of safety against heat sink burnout. Therefore, the prediction of the thermal response of the divertor components is a major concern for both the thermal-hydraulic design and safety analysis of the reactor. Significant work both experimental and theoretical had been carried out in order to investigate the thermal performance of many divertor solutions. Li et al. [6] designed and manufactured three actively cooled tungsten/copper mock-ups with an interlayer made of tungsten–copper

* Corresponding author.
E-mail addresses: selmorshdy@hotmail.com (S.E.-D. El-Morshedy), hassanein@purdue.edu (A. Hassanein).

0920-3796/$ – see front matter © 2010 Elsevier B.V. All rights reserved.
doi:10.1016/j.fusengdes.2010.03.070

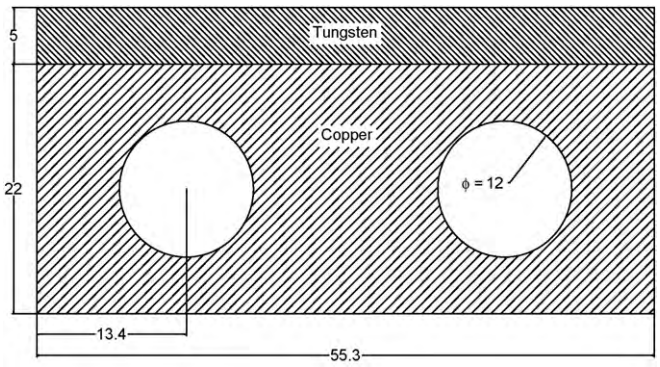

Fig. 1. Flat-tile divertor scheme (dimensions in mm).

alloy (1.5 mm) to study their thermal performance and microstructure analysis for incident heat fluxes up to 5 MW/m^2. Hata and Noda [7] performed numerical thermal analysis on flat-plate divertor made of oxygen-free copper block of 30 mm wide by 25 mm high and heated length from 48 to 149 mm with an armour carbon tile (CX2002U) of 10 mm thickness and cooling tube inner diameter of 10 mm located at a height of 17 mm from the lower surface of the copper block. They also compared the result of their analysis with the experimental data of Kubota et al. [8] on a mock-up divertor plate heated by electron beam facility. Schlosser et al. [9] presented a review of both the flat-tile and mono block divertor solutions and analyzed their assets and drawbacks: pressure drop, critical heat flux, surface temperature and expected behavior during operation, risks during the manufacture, control of armour defects during the manufacture and the reception, and the possibility of repairing defective tiles. They concluded that, the flat-tile concept may deserve more attention as a possible fallback solution to the reference design. In previous work [10], the authors developed a computer code entitled ITERTHA (International Thermonuclear Experimental Reactor Thermal Hydraulic Analysis) based on a transient thermal-hydraulic model to simulate the cooling processes of the ITER divertor in both normal and off-normal operation. The model was benchmarked against experimental data [11,12] performed at Sandia National Laboratory for both bare and swirl-tape coolant channel mock-ups. The code prediction for the thermal behavior of the ITER plasma facing structural materials due to a plasma vertical instability event depositing 60 MJ/m^2 of plasma energy density over 500 ms was also compared with HEIGHTS [13–15]. In the present work, the steady-state analysis of ITERTHA code results is performed and more verification by the commercial finite element code, COSMOS/M [16] is carried out. ITERTHA code is also benchmarked against the thermal-hydraulic calculation of the outer divertor of the Fusion Ignition Research Experiment, FIRE.

2. Calculation description

Fig. 1 shows a cross-sectional view of a flat-tile divertor. The structural material is copper block of 55.3 mm width, 22 mm height, and 1.5 m length coated by 5 mm tungsten tile. The copper block has two cooling channels of 12 mm diameter each located at its horizontal central line. The incident heat on the divertor upper surface is deposited in the divertor structure and removed by a high water flow rate through the cooling channels. It was supposed that, the right, left and lower surfaces of the divertor module are under adiabatic conditions because the divertor is equipped in the plasma vessel. Due to similarity around the vertical axis, the calculation will focus on only one half of the divertor module with only one coolant channel to study the influence of the incident heat flux, swirl-tape insertion and cooling flow velocity on the divertor thermal performance for inlet pressure of 3.6 MPa and inlet temperature of 140 °C.

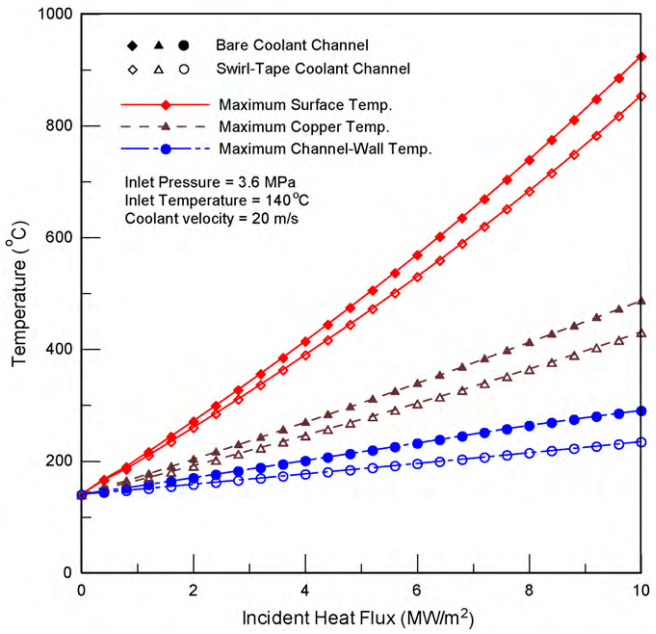

Fig. 2. Divertor temperatures for both bare and swirl-tape channels.

Based on the finite difference technique, ITERTHA solves the heat conduction in the mesh nodes of a half-divertor plate in two-dimensional explicit scheme. 25 elements are chosen in Z direction, 100 points in X direction, and 160 points in Y direction (100 for Cu and 60 for W). Fig. 2 shows the maximum predicted temperature through the divertor of 5 mm tungsten armour for incident heat fluxes up to 10 MW/m^2 and water cooling velocity of 20 m/s. The results are obtained for both bare and swirl-tape coolant channel with swirl-tape ratio of 2 and swirl-tape thickness of 2 mm. By increasing the incident heat flux, the temperatures increased gradually to reach maximum values of 924, 486 and 290 °C for the surface, copper and wall respectively at an incident heat flux of

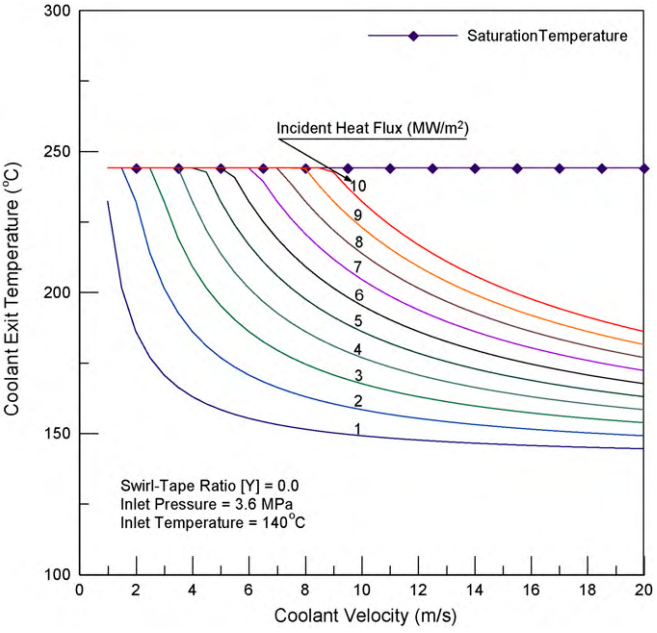

Fig. 3. Divertor exit coolant temperatures under different incident heat fluxes.

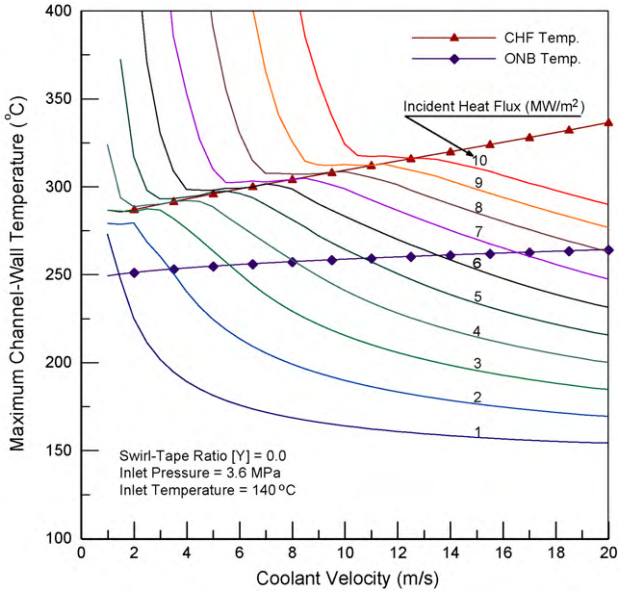

Fig. 4. Divertor maximum channel-wall temperatures under different incident heat fluxes.

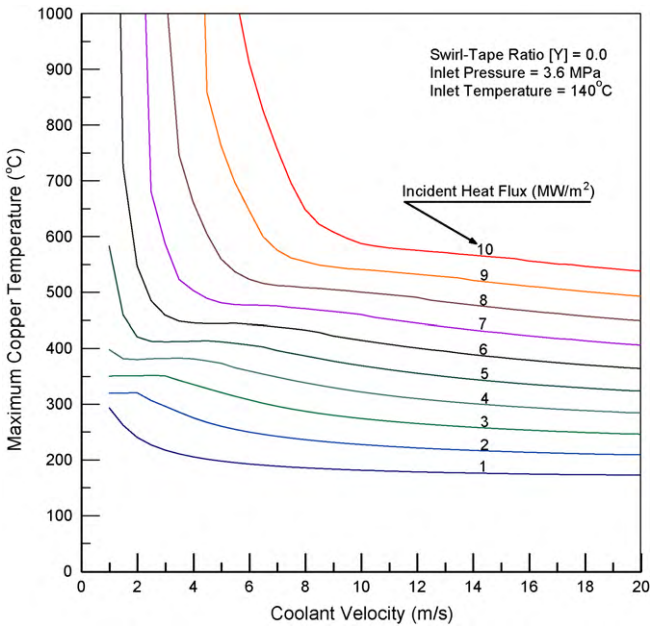

Fig. 5. Divertor maximum copper temperatures under different incident heat fluxes.

10 MW/m^2. The heat transfer process is enhanced due to swirl-tape insertion and so channel-wall temperature reduced. This leads to a reduction in both the copper and tungsten temperatures as shown in Fig. 2. Under this operating condition and an incident heat flux of 10 MW/m^2, the maximum temperature reduction was about 56 °C for channel-wall and copper temperatures and about 71 °C for tungsten surface temperature.

3. Influence of coolant velocity

The coolant velocity is an important parameter affecting the divertor thermal performance. Figs. 3–6 show the coolant temperature, maximum channel-wall temperature, maximum copper temperature, and maximum surface temperature at the divertor exit respectively for a coolant velocity ranges from 1 to 20 m/s

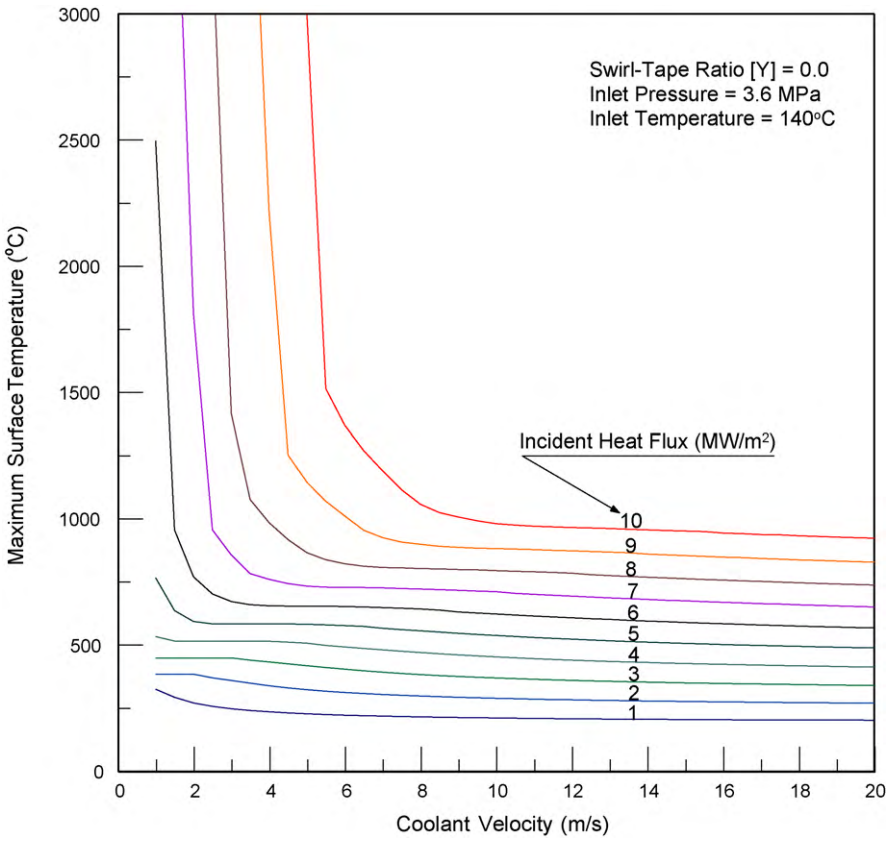

Fig. 6. Divertor maximum surface temperatures under different incident heat fluxes.

under different incident heat fluxes ranges from 1 to 10 MW/m^2. In Fig. 3 the exit coolant temperature is increased by decreasing the coolant velocity, however it remains below the saturation for an incident heat flux of 1 MW/m^2 to be subcooled by about 12 °C for 1 m/s cooling velocity. But the coolant temperature reaches the saturation temperature for heat fluxes equal or greater than 2 MW/m^2. By increasing the incident heat flux, the exit coolant temperature reaches the saturation temperature at higher velocities (for 10 MW/m^2, the exit coolant temperature reaches the saturation for coolant velocities lower than 9 m/s). Fig. 4 shows the maximum channel-wall temperature and the predicted temperatures at both the onset of nucleate boiling and critical heat flux. It shows that for an incident heat flux of 1 MW/m^2 the heat transferred to the coolant by single-phase (liquid) convection regime, while nucleate boiling is achieved for an incident heat flux of 2 MW/m^2 and coolant temperature lower than 3.5 m/s. By increasing the incident heat flux, the channel-wall temperatures achieves onset of nucleate boiling at higher coolant velocities. For an incident heat flux of more than 8 MW/m^2 the channel-wall temperatures achieves onset of nucleate boiling even at a coolant velocity of 20 m/s. Fig. 4 reveals also that, the channel-wall temperature does not achieve burnout for incident heat fluxes lower than 3 MW/m^2. It shows also that, despite of exceeding the Critical Heat Flux (CHF) temperature, the channel-wall temperature decreased or unchanged by reducing the coolant velocity before it increases sharply. At this moment the wall area that is subjected to intense nucleation is much more than that subjected to burnout, this leads to a higher heat transfer coefficient and in tern a lower wall temperature. By decreasing the coolant velocity, the area of burnout becomes more significant and therefore, the channel-wall temperature is increased sharply. Fig. 5 shows the maximum copper temperature predicted at the copper–tungsten interface. It shows that, for incident heat fluxes higher than 5 MW/m^2, the copper structure may melt for coolant velocities lower than 5.5 m/s. While Fig. 6 reveals that tungsten achieves melting for incident heat fluxes higher than 6 MW/m^2 and coolant velocities lower than 5 m/s. For any change in the divertor dimensions and/or inlet coolant pressure and temperature, similar curves in Figs. 3–6 could be generated by ITERTHA code which assists the prediction of the thermal-hydraulic safety margins for coolant saturation, channel-wall burnout, copper melting, and tungsten melting under the selected operating conditions.

4. Verification against COSMOS code

ITERTHA results are verified by the commercial finite element code COSMOS [16] where a two-dimensional triangular mesh of 0.1 mm size is adopted for the divertor plate model at its coolant channel exit. The coolant exit temperature is calculated outside

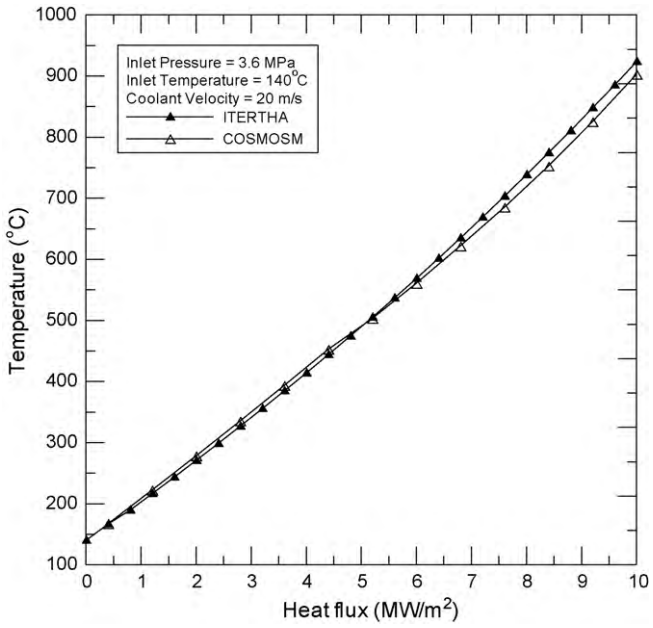

Fig. 7. Divertor maximum surface temperature for various incident heat fluxes.

COSMOS code for each incident heat flux value and submitted to the code and iteration is used to predict the steady-state temperature distribution through the divertor in the following manner:

(1) An arbitrary constant heat transfer coefficient value is assumed at all nodes on the model cooling channel for the first iteration.
(2) COSMOS model is executed to predict the divertor temperature distribution.
(3) The heat flux predicted by COSMOS at each node is used outside the code to predict the corresponding wall temperature values using the same heat transfer models used in ITERTHA.
(4) COSMOS is provided by the wall temperature values predicted by step 3 as a new boundary condition for the next iteration.
(5) COSMOS model is executed again to predict the new divertor temperature distribution.
(6) Steps 3–5 are repeated until the temperature distributions of two successive iterations remains unchanged.

Fig. 7 shows a comparison between the surface temperatures predicted by ITERTHA and COSMOS codes for incident heat fluxes ranging from 1 to 20 MW/m^2. The comparison is performed under the following conditions:

(1) coolant inlet pressure = 3.6 MPa

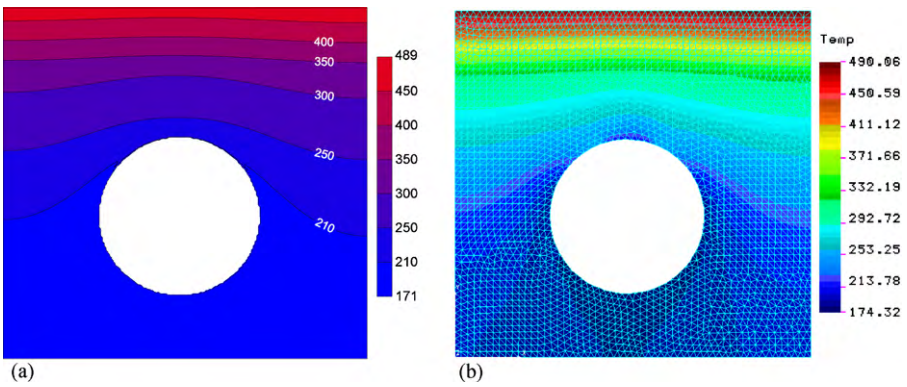

Fig. 8. Divertor temperature distribution at an incident heat flux = 5 MW/m^2. (a) ITERTHA prediction and (b) COSMOS prediction.

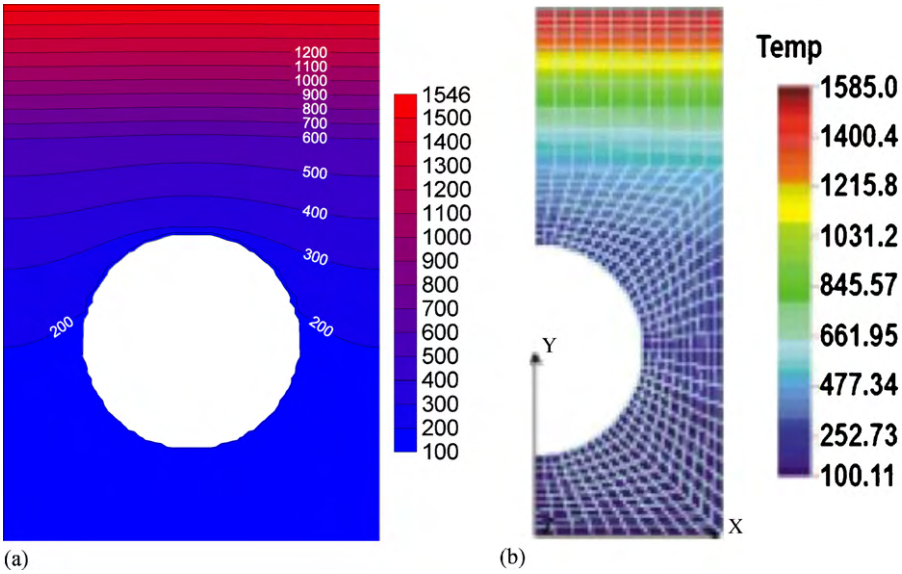

Fig. 9. FIRE divertor temperature distribution at an incident heat flux = 20 MW/m^2. (a) ITERTHA prediction and (b) Baxi prediction.

(2) coolant inlet temperature = 140 °C
(3) coolant velocity = 20 m/s

The comparison shows a very good agreement as shown in Fig. 7. The temperature distribution through the divertor module predicted by ITERTHA and COSMOS at an incident heat flux of 5 MW/m^2 is also shown in Fig. 8(a) and (b), where an excellent agreement is achieved.

5. Benchmarking against previous calculations

In this section, ITERTHA is benchmarked against previous calculations of Baxi et al. [17] for the outer divertor of the Fusion Ignition Research Experiment (FIRE) using COSMOS code [16]. The divertor cell consists of a copper mono block 14 mm × 15 mm with 5 mm tungsten brush as PFC. The comparison is performed under the following conditions:

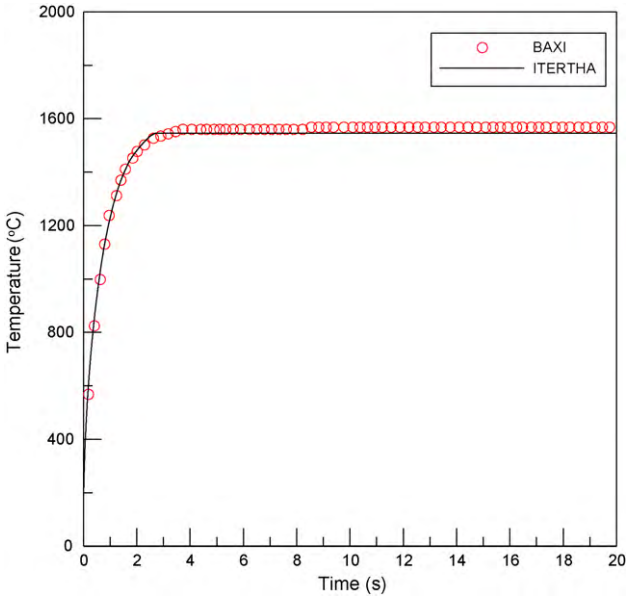

Fig. 10. Transient of the peak surface temperature in FIRE divertor.

(1) incident surface heat flux = 20 MW/m^2
(2) nuclear heating in tungsten = 42 W/cm^3
(3) nuclear heating in copper = 16 W/m^3
(4) coolant flow velocity = 10 m/s
(5) exit coolant temperature = 95 °C
(6) exit coolant pressure = 1.06 MPa
(7) coolant channel diameter = 8 mm
(8) swirl-tape ratio, Y = 2
(9) swirl-tape thickness = 1.5 mm

Fig. 9 shows the temperature distribution of the FIRE divertor predicted by both ITERTHA and Baxi ((a) and (b) respectively) where a very good agreement is achieved. Fig. 10 shows also the transient of the peak surface temperature where it is clear that, ITERTHA calculation is in excellent agreement with Baxi calculation. The results obtained by ITERTHA code for FIRE divertor prove the successful implementation of both the hydraulic and heated diameters of the swirl-tape channels in the heat transfer correlation without involving any additional factors in the original correlations.

6. Conclusion

An analytical study using the International Thermonuclear Experimental Reactor Thermal Hydraulic Analysis (ITERTHA) code is performed to investigate the influence of the incident heat flux, swirl-tape insertion in cooling channels as well as the coolant flow velocity on the thermal response of a divertor of copper heat sink with 5 mm tungsten armour. The ITERTHA code results are verified by the commercial finite element code, COSMOS using the same methodology for obtaining the heat transfer coefficients at the nodes located on the cooling channel. A very good agreement is achieved under different incident heat fluxes up to 20 MW/m^2. The ITERTHA code is also benchmarked against the thermal-hydraulic calculation of the outer divertor of the Fusion Ignition Research Experiment, FIRE with swirl-tape cooling channel for an incident heat flux of 20 MW/m^2, coolant flow velocity of 10 m/s, with swirl-tape ratio of 2 and swirl-tape thickness of 1.5 mm. The results show a very good agreement for both steady and transient states and prove not only the efficiency of the calculation methodology but also the successful implementation of both the hydraulic and heated diameter of the swirl-tape channels in the used heat transfer correlations without involving any additional factors in the original

correlations. In addition, ITERTHA code is very easy to run and very fast to execute on various platforms.

Acknowledgment

This work is supported by the U.S. Department of Energy, Office of Fusion Energy Sciences.

Appendix A. ITERTHA calculation method

A.1. Coolant temperature

The coolant channel is divided into a given number of elements in the axial Z direction where the general energy balance equation is applied to each element:

$$\rho A dz \frac{dI}{d\tau} = \int_0^{2\pi} \phi(\theta)\ d\theta\, R\, dz - GA(I_{in} - I_{out}) \tag{A1}$$

where A is the channel cross-sectional area, $\phi(\theta)$ is the wall heat flux at radial angle θ, R is the coolant channel radius, G is the coolant mass flux, and I is the coolant enthalpy.

A.2. Divertor temperature

The temperature distribution through the divertor is calculated by solving the general heat conduction equation by the finite difference technique in two-dimensional explicit scheme.

$$\rho Cp \frac{dT}{d\tau} = \frac{\partial}{\partial x}\left(K(T)\frac{\partial T}{\partial x}\right) + \frac{\partial}{\partial y}\left(K(T)\frac{\partial T}{\partial y}\right) + q(x, y, \tau) \tag{A2}$$

where K is the thermal conductivity.

A.3. Coefficient of heat transfer

The heat transfer coefficient for both the single-phase and the boiling two-phase flow is obtained as follows.

A.3.1. Single-phase forced convection

(a) Turbulent regime Re ≥ 10,000; Dittus and Boelter [18] equation is used:

$$\mathrm{Nu} = 0.023\ \mathrm{Re}^{0.8}\mathrm{Pr}^{0.4} \tag{A3}$$

(b) Transition regime 2100 < Re < 10,000; Nusselt number is calculated by interpolation between the laminar and turbulent correlations.

(c) Forced laminar regime Re ≤ 2100; Sieder and Tate [19] correlation is used:

$$\mathrm{Nu} = 1.86\left(\frac{\mathrm{Re}\ \mathrm{Pr}}{L/D_e}\right)^{1/3}\left(\frac{\mu_c}{\mu_w}\right)^{0.14} \tag{A4}$$

A.3.2. Subcooled boiling

Boiling is initiated when the coolant channel-wall temperature is equal to the onset of nucleate boiling temperature, T_{ONB}, where

$$T_{ONB} = T_{sat} + (\Delta T_{sat})_{ONB} \tag{A5}$$

where $((T_{sat})_{ONB}$ is given by Bergles and Rohsenow correlation [20] which is valid for water only over the pressure range 1–138 bar:

$$(\Delta T_{sat})_{ONB} = 0.556\left\{\frac{\phi_{ONB}}{1082P^{1.156}}\right\}^{0.463P^{0.0234}} \tag{A6}$$

where P is the local pressure in bar and ϕ_{ONB} is in W/m^2.

The correlation developed by Chen [21] for saturated boiling as described subsequently is extended for use in the subcooled boiling. It is assumed that the total heat flux is made up of a nucleate boiling contribution and a single-phase forced convective contribution.

$$\phi(z) = h_{NCB}(T_w(z) - T_{sat}(z)) + h_{SP}(T_w(z) - T_c(z)) \tag{A7}$$

where h_{SP} is calculated as described in Section A.3.1 and h_{NCB} is calculated for saturated boiling detailed in the next section.

A.3.3. Saturated nucleate boiling

The heat transfer coefficient in forced flow saturated boiling is calculated by the correlation proposed by Chen [21]:

$$h_{TP} = h_{SP} + h_{NCB} \tag{A8}$$

$$h_{SP} = 0.023\left[\frac{G(1-x)D_e}{\mu_l}\right]^{0.8}\left[\frac{\mu Cp}{k}\right]_l^{0.4}\left(\frac{k_l}{D_e}\right)(F) \tag{A9}$$

F is the convective boiling enhancement factor and calculated as:

$$F = \begin{cases} 1.0 & \text{for } \dfrac{1}{X_{tt}} \le 0.1 \\ 2.35\left(\dfrac{1}{X_{tt}} + 0.213\right)^{0.736} & \text{for } \dfrac{1}{X_{tt}} > 0.1 \end{cases} \tag{A10}$$

where X_{tt} is the Lockhart–Martinelli parameter and given by:

$$X_{tt} = \left(\frac{1-x}{x}\right)^{0.9}\left(\frac{\rho_g}{\rho_l}\right)^{0.5}\left(\frac{\mu_l}{\mu_g}\right)^{0.1} \tag{A11}$$

$$h_{NCB} = 0.00122\left[\frac{k_l^{0.79}Cp_l^{0.45}\rho_l^{0.49}}{\sigma^{0.5}\mu_l^{0.29}I_{fg}^{0.24}\rho_g^{0.24}}\right]\Delta T_{sat}^{0.24}\Delta P_{sat}^{0.75}(S) \tag{A12}$$

where ΔT_{sat} is the wall superheat, ΔP_{sat} is the difference between the saturation pressures calculated from the wall temperature and the fluid temperature and S is the nucleate boiling suppression factor and calculated as:

$$S = \begin{cases} \left[1 + 0.12\mathrm{Re}_{TP}^{1.14}\right]^{-1} & \text{for } \mathrm{Re}_{TP} < 32.5 \\ \left[1 + 0.42\mathrm{Re}_{TP}^{0.78}\right]^{-1} & \text{for } 32.5 < \mathrm{Re}_{TP} < 70 \end{cases} \tag{A13}$$

Re_{TP} is the two-phase Reynolds number and given by:

$$\mathrm{Re}_{TP} = \mathrm{Re}_l \times F^{1.25} \tag{A14}$$

A.3.4. Transition film boiling

Tong-75 correlation [22] is used to calculate the critical heat flux as it is satisfactory incorporates the thermal and hydrodynamic effects associated with the onset and progression of CHF. Its predictions for the local CHF has been recommended for fusion CHF as it compares well with experimental data.

$$\phi_{CHF} = 0.23 f_0 G I_{fg}(1 + 0.00216P_{ratio}^{1.8}\mathrm{Re}^{0.5}\mathrm{Ja}) \tag{A15}$$

where f_0 is the Fanning friction factor; $f_0 = 8.0\mathrm{Re}^{-0.6}D_{ratio}^{0.32}$, $D_{ratio} = D_e/D_0$; D_e is the hydraulic diameter and D_0 is a reference diameter = 0.0127 m, $P_{ratio} = P/P_c$; P is the local pressure and P_c is the critical pressure = 22.1 MPa, Ja is the Jakob number; Ja = $-X_{sub}(\rho_l/\rho_g)$ and X_{sub} is the quality of subcooled liquid; $X_{sub} = (-Cp\Delta T_{sub}/I_{fg})$.

As the wall temperature reaches the CHF temperature (the wall temperature at a heat flux = ϕ_{CHF}) the model calculates the heat transfer coefficient using Marshall-98 correlation [23] as it demonstrated agreement with data from fusion-relevant experiments.

$$\phi = \phi_{CHF}\left(\frac{T_w - T_{sat}}{T_{CHF} - T_{sat}}\right)^{-0.23} \tag{A16}$$

A.4. Heat transfer enhancement

A.4.1. Forced convection heat transfer

The value of Nusselt number given in Section A.3.1 is multiplied by the swirl-tape modification of Lopina and Bergles [24] as follows:

$$\mathrm{Nu}_{st} = \mathrm{Nu} \times 2.26Y^{-0.248} \tag{A17}$$

where Y is the swirl-tape ratio, defined as the number of tube inner diameters per the pitch length for 180° rotation of the tape.

A.4.2. Critical heat flux

The critical heat flux correlation for bare tubes (Tong-75 correlation) is also used for swirl-tape tubes after modifying its friction factor by Lopina and Bergles [24] to account for the swirl-tape inserts.

$$f_{st} = f_0 \times [2.75Y^{-0.406}] \tag{A18}$$

where f_{st} is the friction factor for swirl-tape tube.

For swirl-tape tubes the concept of the equivalent hydraulic diameter is applied to all the previous heat transfer correlations while the concept of the heated diameter is applied to the energy equation. The equivalent hydraulic diameter takes the following form:

$$D_e = 4 \times \left[\frac{(\pi D^2/4) - \delta D}{\pi D + 2(D - \delta)}\right] \tag{A19}$$

while the heated diameter takes the following form:

$$D_h = 4 \times \left[\frac{(\pi D^2/4) - \delta D}{\pi D - 2\delta}\right] \tag{A20}$$

where δ is the tape thickness.

References

[1] M. Araki, M. Ogawa, T. Kunugi, K. Satoh, S. Suzuki, Experiments on heat transfer of smooth and swirl tubes under one-sided heating conditions, International Journal of Heat and Mass Transfer 39 (14) (1996) 3045–3055.

[2] T. Marshall, Safety implications of an integrated boiling curve model for water-cooled divertor channels, Fusion Engineering and Design 63–64 (2002) 235–242.

[3] J. Boscary, J. Fabre, J. Schlosser, Critical heat flux of water subcooled flow in one-side heated swirl tubes, International Journal of Heat and Mass Transfer 42 (1999) 287–301.

[4] G. Janeschitz, Plasma wall interaction issues in ITER-FEAT, in: 14th-PSI, Plasma Surface Interaction Conference, Rosenheim, May, 2000.

[5] Draft Report for ITER Concept Definition Phase, IAEA, ITER Technical Report, 1989.

[6] H. Li, J.L. Chen, J.G. Li, X.J. Sun, High heat load tests on W/Cu mock-ups and evaluation of their application to EAST device, Fusion Engineering and Design 84 (2009) 1–4.

[7] K. Hata, N. Noda, Thermal analysis on flate-plate-type divertor based on subcooled flow boiling critical heat flux data against inlet subcooling in short vertical tube, Journal of Heat Transfer 128 (2006) 311–317.

[8] Y. Kubota, N. Noda, A. Sagara, A. Komori, N. Inoue, K. Akaishi, H. Suzuki, N. Ohyabu, O. Motojima, Development of high heat flux components in large helical device (LHD), in: Proceeding of the ASME Heat Transfer Division, HTD-vol. 317-1, IMECE, 1995, pp. 159–163.

[9] J. Schlosser, F. Escourbiac, M. Merola, S. Fouquet, P. Bayetti, J.J. Cordier, A. Grosman, M. Missirlian, R. Tivey, M. Rodig, Technologies for ITER divertor vertical target plasma facing components, Nuclear Fusion 45 (2005) 512–518.

[10] S.E.-D. El-Morshedy, A. Hassanein, Transient thermal-hydraulic modeling and anlysis of ITER divertor plate system, Fusion Engineering and Design 84 (December (12)) (2009) 2158–2166.

[11] T.D. Marshall, Experimental Examination of the Post-Critical Heat Flux and Loss of Flow Accident Phenomena for Prototypical ITER Divertor Channels, PhD Thesis, Rensselaer Polytechnic Institute, Troy, New York, 1998.

[12] T.D. Marshall, J.M. McDonald, L.C. Cadwallader, D. Steiner, An experimental examination of the loss of flow accident phenomenon for prototypical ITER divertor channels of $Y = 0$ and $Y = 2$, Fusion Technology 37 (2000) 38–53.

[13] A. Hassanein, Prediction of material erosion and lifetime during major plasma instabilities in Tokamak devices, Fusion Engineering and Design 60 (2002) 527–546.

[14] A. Hassanein, T. Sizyuk, Comprehensive simulation of vertical plasma instability events and their serious damage to ITER plasma facing components, Nuclear Fusion 48 (2008), 115008 (11 pp).

[15] A. Hassanein, T. Sizyuk, M. Ulrickson, Vertical displacement events: a serious concern in future ITER operation, Fusion Engineering and Design 83 (2008) 1020–1024.

[16] COSMOS/M, A Finite Element Analysis Code, Structural Research and Analysis Corporation, Santa Monica, California, USA.

[17] C.B. Baxi, M.A. Ulrickson, D.E. Driemeyer, P. Heitzenroeder, Thermal Hydraulic Analysis of FIRE Divertor, GA-A23494, October 2000.

[18] F.W. Dittus, L.M.K. Boelter, University of California, Berkeley, Publications on Engineering, vol. 2, 1930, p. 443.

[19] E.N. Sieder, G.E. Tate, Industrial and Engineering Chemistry 28 (1936) 1429.

[20] J.G. Collier, Convective Boiling and Condensation, second ed., McGraw-Hill Internal Book Company, 1981.

[21] J.C. Chen, A correlation for boiling heat transfer to saturated fluids in convective flow, Industrial and Engineering Chemistry, Process Design and Development 5 (3) (1966) 322–329.

[22] L.S. Tong, A Phenomenological Study of Critical Heat Flux, ASME paper, 75-HT-68.

[23] J.A. Koski, R.D. Watson, A.M. Hassanein, P.L. Goranson, J.C. Salmonson, Thermal-hydraulic design issues and analysis for the ITER divertor, Fusion Technology 19 (1991) 1729–1735.

[24] R.F. Lopina, A.E. Bergles, Heat transfer and pressure drop in tape-generated swirl flow of single phase water, Journal of Heat Transfer 91 (8) (1969) 434–442.